Clays and Clay Minerals, Vol. 40, No. 4, 387–396, 1992.

X-RAY DIFFRACTION STUDIES OF ILLITE/SMECTITE FROM ROCKS, <1 μm RANDOMLY ORIENTED POWDERS, AND <1 μm ORIENTED POWDER AGGREGATES: THE ABSENCE OF LABORATORY-INDUCED ARTIFACTS

R. C. REYNOLDS, JR.

Department of Earth Sciences, Dartmouth College, Hanover, New Hampshire 03755

Abstract—X-ray diffraction patterns were obtained from rock fragments, <1 μm randomly oriented freeze-dried powders, and <1 μm oriented aggregates for 11 mixed-layered illite/smectite samples (K-bentonites) that cover the range from 14 to 100 percent expandable. In all cases, 00*l* and *hkl* comparisons show no evidence of laboratory induced artifacts. Either the laboratory procedures caused no disaggregation of fundamental illite particles, or, if they did, fundamental particle reaggregation during sample preparation duplicated the one and three-dimensional structures of the illite/smectite in the original, untreated rock.

Demodulation of the 20*l*, 13*l* reflections into a two-dimensional band shape occurred with increasing percent expandable layers in illite/smectite. This result strongly supports the contention that turbostratic displacements occur at the expandable interfaces between fundamental particles, and are limited to those sites.

A comparison of the quantities measured by powder X-ray diffraction and high resolution transmission electron microscope (TEM) lattice fringe image techniques for disordered crystals suggests that meaningful comparisons between the two methods can be made only if a sufficient number of images are recorded to define the statistical parameters of the disorder.

Key Words—Artifacts, Illite/smectite, Powder X-ray diffraction, Sample preparation, Turbostratic, X-ray coherence.

INTRODUCTION

Mixed-layered illite/smectite (I/S) is traditionally thought of as a mixture of crystallites that contain illite and smectite as two distinct, interstratified mineral entities. Similar atomic geometry in the surface oxygen planes of the tetrahedral sheets makes it likely that a good fit exists at the 001 cleavage interfaces between these two minerals. I/S crystals should be robust and, like other minerals, should not be easily broken down into planar fragments that approach one unit cell in thickness. Nor should it be possible to reassemble them after such disaggregation. Norrish (1954) demonstrated that Na-montmorillonite could be so dispersed by osmotic swelling, but no one until recently associated such properties with I/S.

In 1984, Nadeau and others (1984a, 1984b, 1984c) demonstrated that simple dispersion of sodium-saturated I/S caused the separation of I/S crystallites into exceedingly thin particles. Depending on the illite content of the megascopic aggregate these particles contained one, two, or (at most) a few 10-Å layers. More importantly, the researchers were able to reaggregate these ultra-dispersed sols into X-ray coherent stacks of perhaps 10 or more unit silicate layers. They called the thin stacks of 10-Å layers fundamental illite particles, and argued that what had been considered smectite was actually the expandable interface between illite fundamental particles.

Their findings suggested to some that the commonly used methods for preparing oriented aggregates for powder X-ray diffraction (XRD) analysis had introduced artifacts into much of the published data on I/S. Perhaps XRD data were comparable only among laboratories that used identical sample preparation methods. A few (e.g., Ransom and Helgeson, 1989) went farther and implied that clay scientists might not know the nature of I/S in rocks because the accumulated lore was based on artifactual crystal structures that could be very different from the natural ones.

Two types of artifacts could be produced in the laboratory. The first is the modification of the stacking sequences that control ordering, or lack thereof, in the organization of unit cells or unit layers along the *Z* direction. The second could change the registry of the mica-like stacks with respect to each other, introducing or increasing the incidence of turbostratic defects.

The first type of artifact is inconsistent with the fundamental particle concept, and the argument is presented later. The second kind of artifact is not so easy to dismiss. Powder XRD experiments reported here suggest that the interfaces between fundamental particles are turbostratic in the rock and in the separated clay-sized aggregate, but these findings are at variance with HRTEM (high resolution transmission electron microscope) lattice fringe image studies by Veblen *et al.* (1990) and Ahn and Buseck (1990).

The purpose of this study is to explore the nature of artifacts, if any, produced by commonly used non-aggressive and minimal sample preparation procedures. Powder XRD studies were conducted on I/S

Table 1. Samples studied. All are bentonites except for the Zempleni clay which is a hydrothermally altered rhyolite.

Sample	Percent exp.	Reich-weite	Age and location
Umiat[1]	100	—	Cretaceous, Alaska
MB 405[2]	80	0	Cretaceous, Utah
MB 254[2]	60	0	Cretaceous, Colorado
G3SH[3]	54	0	Devonian, Gaspé, Quebec
SA 7b[4]	31	1	Cretaceous, Montana
SA 9	25	1	Cretaceous, Montana
GLRD[3]	19	1.5	Devonian, Gaspé, Quebec
Zempleni[5]	14	3	Hydrothermal, Hungary

[1] Anderson and Reynolds, 1966.
[2] Nadeau and Reynolds, 1981.
[3] Smith, 1967.
[4] Altaner *et al.*, 1984.
[5] Provided by J. Środoń.

minerals prepared by two sample preparation procedures selected to represent possible extremes in the styles of fundamental particle reaggregation. The results are compared in each case (except one) with the baseline standard provided by XRD analysis of the bulk, unground rock.

EXPERIMENTAL

Samples

Fourteen samples of K-bentonite, one bentonite, and one hydrothermally altered rhyolite were studied. Of these, eight were selected to illustrate the findings reported here, although the ones not described showed no characteristics different from the others. Table 1 gives some relevant information on the samples.

Rock: preparation

Diffraction data for the rock fragments are crucial to the conclusions of this study. The most unaggressive procedure possible was used to minimize anticipated criticisms that the diffraction data contain artifacts. The label "rock" is used to underscore the fact that the sample received minimal treatment before XRD analysis.

Fragments of bentonite, K-bentonite, or hydrothermal clay were selected that ranged from 0.5 cm to 3 cm in average dimension. Fragments were chosen that contained relict bedding to ensure that the rock had not been turbated naturally in outcrop. The fragments were dropped into a teflon mold containing a thin layer of epoxy and the preparation was removed after curing. The sample mount was inverted and lightly ground to a flat surface on #400 carborundum paper. Its surface was then blown clear of dust. The preparation was exposed to ethylene glycol vapor for 24 hr at 60°C and analyzed on the diffractometer over the angular range of 2 to 44° 2θ. Some specimens were single blocks, and others were mosaics. Interestingly, ethylene glycol solvation caused none of the preparations to swell enough to disrupt their original shapes.

<1 μm fraction: random powder preparation

Portions of each sample were dispersed in distilled water by means of an industrial grade Waring blender followed by treatment with ultrasound. The suspensions were washed to incipient dispersion by centrifuging in repeated changes of distilled water. Dispersion was completed by making the suspension 0.005 M with respect to sodium pyrophosphate, and the <1 μm fraction e.s.d. was extracted by centrifugation. The suspension was concentrated to about 1 percent clay by ultracentrifugation, frozen in a Labconco shell freezer (−30°C), and lyophyllized in a Labconco 4.5 freeze drier. The freeze-dried powder was lightly ground with a rubber stopper mounted on a glass rod, spread in an evaporating dish, and exposed for 24 hr to ethylene glycol vapor at 60°C. The powder was prepared for XRD analysis by the side-loading procedure. The combination of freeze-drying and side-loading produced excellent examples of random orientation.

The Umiat Bentonite (Table 1) was not freeze-dried because attempts to do so produced a leathery, oriented film that could not be ground to a powder. The <1 μm fraction was collected by ultracentrifugation, dried at 60°C, ground in an alundum mortar, solvated with ethylene glycol and side-loaded for analysis.

Sample MB 405 (Table 1) consists of fragments too fine to allow the preparation of an epoxy mosaic. The bulk sample was hand ground for analysis.

<1 μm fraction: oriented aggregate preparation

Portions of the freeze-dried powder were redispersed in distilled water by means of ultrasonic disaggregation. The suspension was pipetted onto a glass slide, dried at 90°C, and ethylene glycol-solvated as described above. The concentration of the suspension was controlled to ensure that the weight of clay on the dried slide exceeded 20 mg per cm^2.

X-ray diffraction analysis

All diffraction data were obtained with a Siemens D-500 diffractometer equipped with Cu tube and a diffracted beam graphite monochrometer. The geometry consisted of a diffracted beam Soller slit (2°), and 1° beam and 0.15° detector slits. Step scans were made by computer control at 2θ increments of 0.05°. Count times per step were 20 s for the rock and random powder preparations and 5 s for the oriented aggregates. After each run, the low-angle regions were again recorded to insure that evaporation of ethylene glycol during the analysis had been insufficient to alter the diffraction results. This procedure was carried out only a few times because it quickly became evident that evaporation of ethylene glycol presented no problems.

Low-angle intensity corrections

Diffraction data require correction for air scatter, sample length differences, and Lorentz factor differences if valid comparisons are to be made among the different sample preparations.

Summarizing Ergun's work, Klug and Alexander (1974) give the air scatter (a_r) received by the detector, in the absence of a specimen and for the symmetrical-reflection geometry, as

$$a_r = \frac{1}{2} + \left(\frac{1}{2} - \frac{T \cos\theta}{R\beta}\right)\exp\left(\frac{-2\mu T}{\sin\theta}\right).$$

T is the sample thickness, R is the goniometer radius, β is the angle subtended by the detector slit, θ is the diffraction angle, and μ is the sample absorption coefficient. This equation applies to a very thin sample film that allows appreciable penetration by the incident beam and thus allows a significant contribution from air scatter produced by the air volume behind the sample. However, all of the present data were collected from sample films that were effectively infinitely thick and backed up by either a glass slide or an aluminum substrate. Consequently, T is so large that the quantity $\exp(-2\mu T/\sin\theta)$ approaches zero, leading the relation $a_r = 1/2$.

Air scatter was measured by recording the intensity (in counts per second) at low diffraction angles with an empty sample holder, and dividing that value by two, in accordance with the correction described above. The air scatter contributions were subtracted from the intensity data files of the random powders and rock preparations, but not from the diffraction patterns of the oriented aggregates; low-angle intensity for the latter was so large that the air scatter contribution was judged to be insignificant.

The length of each rock preparation was measured. The lengths of the side-loaded random powders and oriented aggregates were constant at 3.5 cm and 4.5 cm, respectively. A low-angle intensity correction was applied to make them all equivalent to a 4.5 cm sample length (see Moore and Reynolds, 1989).

The integrated intensity of the I/S 003/005 reflection from each oriented aggregate was used to measure its preferred orientation (Reynolds, 1986). The random powder Lorentz factor was removed by division from the air-scatter-corrected data files for the corresponding rock and random powders, and the Lorentz factor for the oriented aggregates was applied to the diffraction data of these files. The corrections were made only for the low-angle 00*l* comparisons shown in Figures 1 and 2.

The overall effect of the corrections is large, in some cases amounting to a factor of 2 or 3 at 2° 2θ. Small errors cause significant distortions of the extreme low-angle diffraction patterns. For example, discrepancies are present in the low-angle traces for two of the samples (the 54% and 45% expandable minerals in Figure 1). But given the weighty nature of the corrections, errors of 10% or so are not surprising at the extreme lower ranges of 2θ, and that is all that is required to account for the discrepancies shown in Figure 1.

Removal of quartz interference

Bulk rock specimens contain significant amounts of quartz, calcite, zeolite, and feldspar, whose peaks interfere with many of the illite reflections. A peak-stripping algorithm was used to remove the quartz reflections, but it performed poorly on the other minerals and was not used for them. Small residual intensities are left on one or both flanks of the quartz peak positions on some diffraction patterns.

RESULTS

The low-2θ region: basal reflections

Figures 1 and 2 show low-2θ diffraction patterns for the I/S samples. Vertical lines mark the positions of diagnostic I/S peaks. The patterns are so similar among each of the three preparations that identical values for percent expandability and Reichweite were obtained, within the errors of measurement. In addition, measured peak breadths for the illite/smectite 002/003 reflections for each of the three are comparable, suggesting that mean crystallite thicknesses are similar. There is no evidence for laboratory-induced effects on the 00*l* diffraction patterns of these I/S minerals.

Three-dimensional reflections

Figures 3 and 4 show X-ray diffraction patterns for the intermediate-2θ region. Interferences by other minerals in the rock preparations are extreme for some samples, but most of the pairs show similar 11*l* and 02*l* reflections, which convey information on polytypes and their degree of order/disorder. There is no evidence of sample preparation effects on these reflections, and hence no evidence of polytype modification caused by sample preparation.

Using the criteria of Bailey (1980), samples G3SH (45% expandable), GLRD (19% expandable), and Zempleni (14% expandable) are 1*M* or somewhat disordered 1*M* polytypes. SA 4b (31% expandable) and SA 9 (25% expandable) could be 3*T* polytypes or twinned 1*M* varieties, which are almost indistinguishable by powder XRD criteria (Güven and Burnham 1967). Alternatively, they could be 1*M* polytypes based on the octahedral cis-vacant mica unit cell described by Tsipursky and Drits (1984), and illustrated by calculated patterns for micas by Drits *et al.* (1984). Regardless of the interpretation, the broad 11*l* and 02*l* reflections indicate the presence of n.60 or n.120 rotational stacking disorder.

The breadths of the 20*l*, 13*l* peaks (between 34.5 and 39° 2θ) are unaffected by polytypic modifications ($\pm$120°

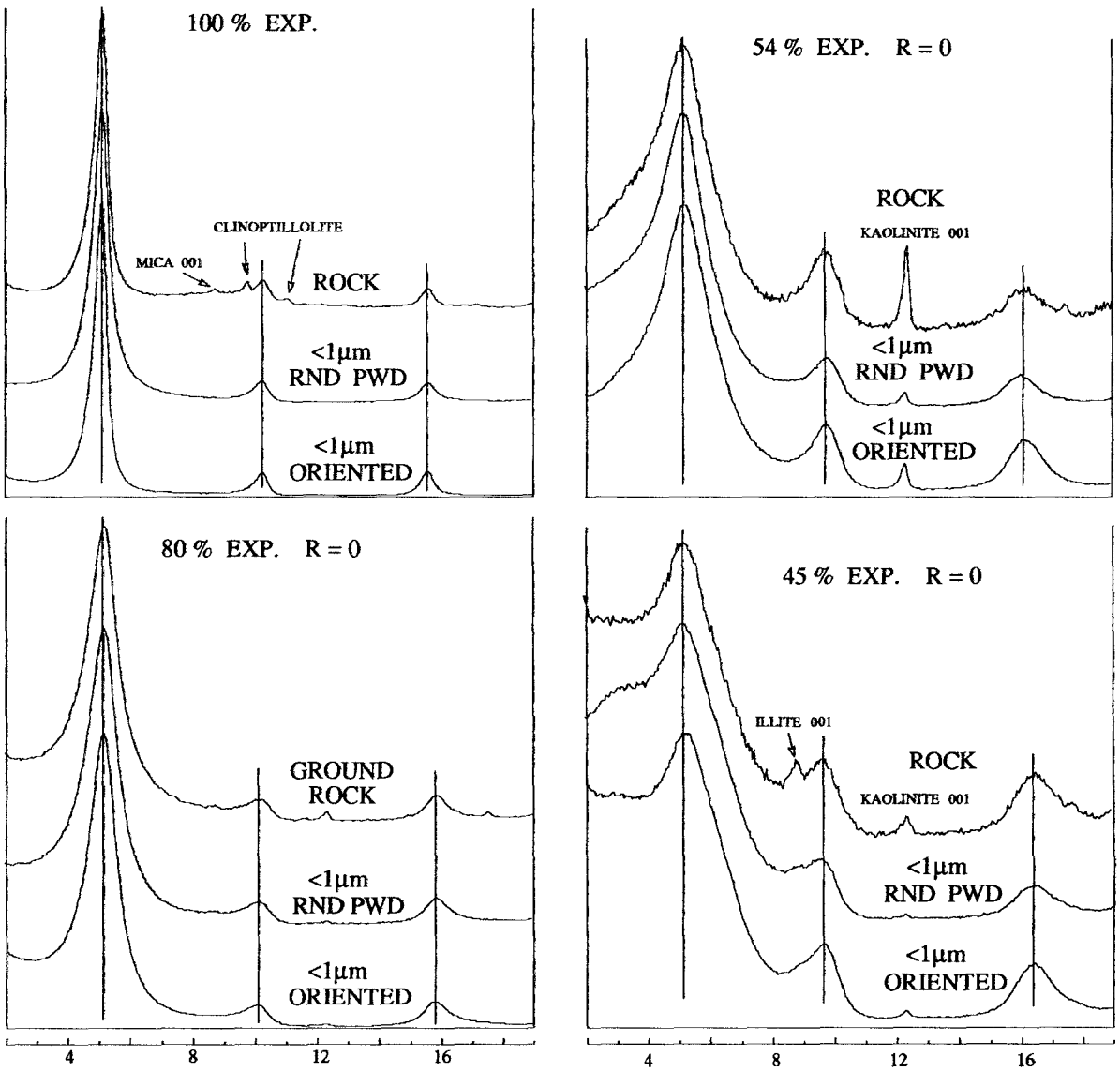

Figure 1. 00*l* diffraction patterns of I/S. Comparisons among rock fragments (rocks), <1 μm freeze-dried powders (<1 μm rnd pwd), and oriented, <1 μm aggregates (<1 μm oriented). Vertical lines mark diagnostic I/S 00*l* reflections. Captions refer to percent expandability and the Reichweite. Degrees 2θ, CuKα.

rotations), but they are broadened by turbostratic disorder along c^*. Turbostratic displacements between each 2:1 silicate layer produce the characteristic 20; 13 band shown by the 100% expandable mineral (Figure 3). But thin zones of illite in I/S (2, 3, etc., unit cells thick) cause the superposition of very broad $k = 3n$, $l > 0$ peaks (marked on Figures 3 and 4) on the band. More illitic compositions contain thicker internally coherent illite stacks, which produce sharper $k = 3n$, $l > 0$ reflections that are better resolved from the band whose characteristic shape disappears entirely for a hypothetical R = 1 or R > 1 structure.

Figures 3 and 4 show no significant differences in the 20*l*, 13*l* region between the rock preparations and the corresponding <1 μm freeze-dried specimens, indicating that sample preparation has not affected the incidence of turbostratic disorder in these minerals.

The demodulation of discrete peaks into the 20; 13 band can be described by a parameter that is sensitive to the frequency of turbostratic stacking defects (the turbostratic index—TSI). It was conceived and is applied in a fashion similar to the Hinckley Index for kaolinite (Hinckley, 1963). Figure 5 shows how the TSI is measured.

The TSI is mostly a measure of the frequency of turbostratic displacements in a mica stacking sequence

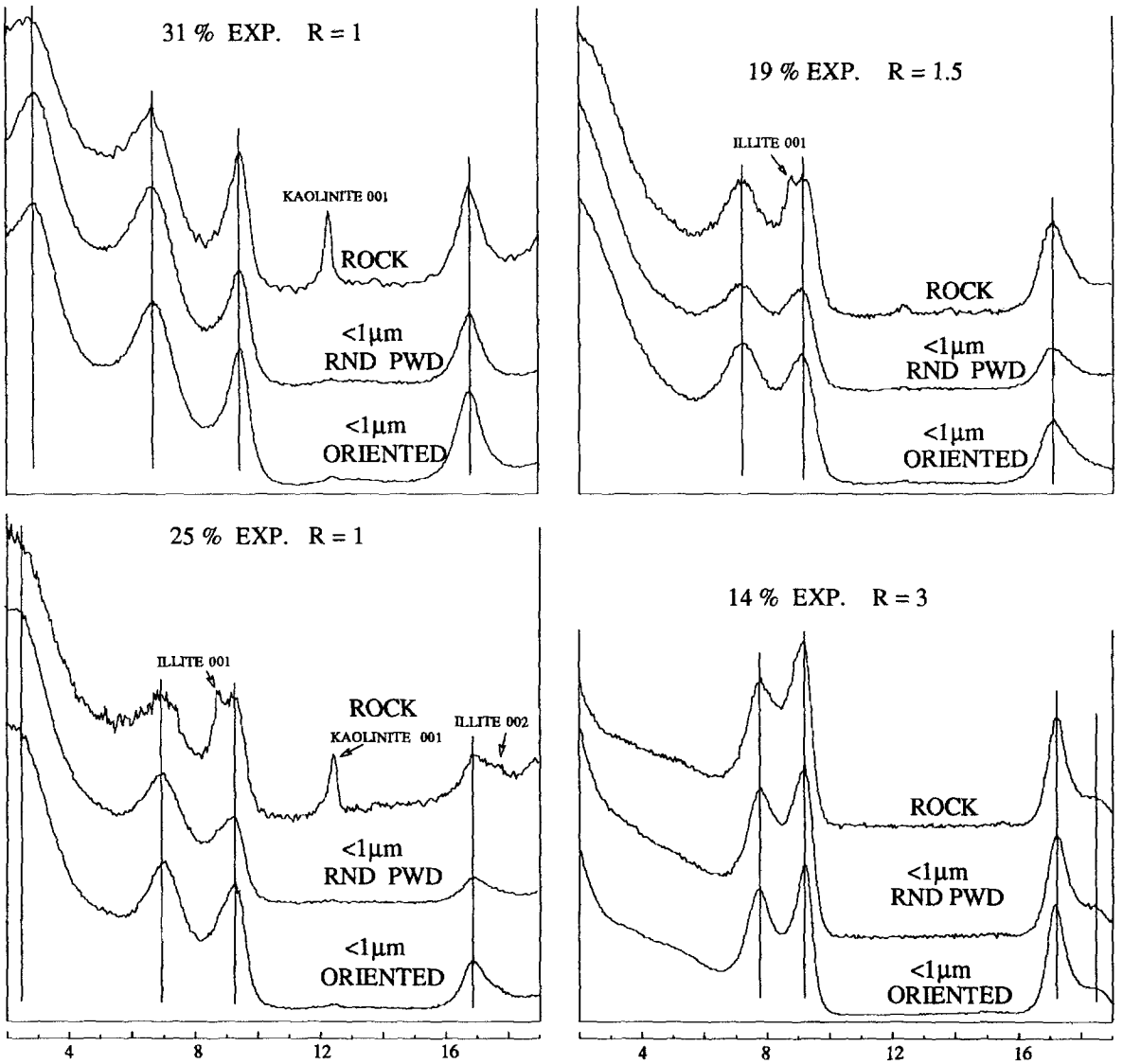

Figure 2. 00*l* diffraction patterns of I/S. Comparisons among rock fragments (rocks), <1 μm freeze-dried powders (<1 μm rnd pwd), and oriented, <1 μm aggregates (<1 μm oriented). Vertical lines mark diagnostic I/S 00*l* reflections. Captions refer to percent expandability and the Reichweite. Degrees 2θ, CuKα.

along c^*, but there are other factors that can complicate its interpretation. The $\bar{2}02$; 131 composite reflection at 36.5° 2θ is weakened by increased concentrations of octahedral iron, thus affecting the saddle at about 35.5° 2θ that is part of the measurement. Bailey (1991) has pointed out that the two composite reflections at 36.5 and 37.6° are resolved into four, if the monoclinic angle is typical of the 1*M* polytype (101.3°) and the crystals are large enough. These reflections and the composite 20*l*; 13*l* peak at 35° are broadened by small particle size. The enhanced breadths of all, together with their separations, raise the saddle and decrease the height of the 201; $\bar{1}32$. In addition, partial orientation within the powder sample may enhance the normally weak 004 reflection that lies exactly on the saddle.

These factors do not, however, create the typical two-dimensional band shape—only turbostratic defects do that. Consequently,the TSI seems suitable for the interpretation placed on it here.

Figure 6 shows a plot of TSI values for the freeze-dried powders *vs* percent expandability determined from 1/S 001/002 and 002/003 peak positions that were obtained from ethylene glycol-solvated, oriented aggregates (Reynolds and Hower, 1970; Reynolds, 1980). The relation indicates a very high degree of correlation between percent expandability and frequency of tur-

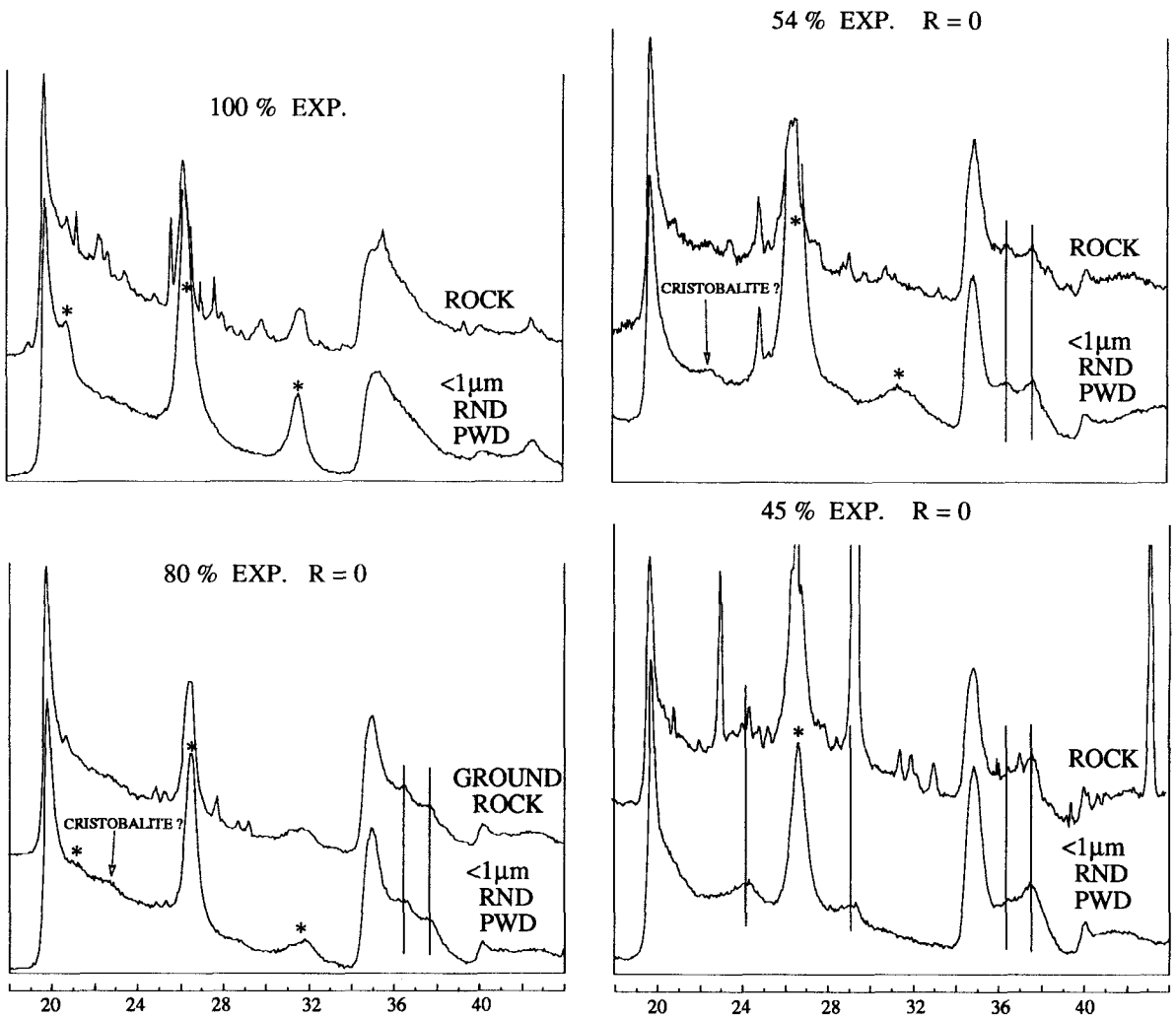

Figure 3. Three-dimensional diffraction patterns of I/S. Comparison between rock fragments (rocks) and <1 μm freeze-dried powders (<1 μm rnd pwd). Captions refer to percent expandability and the Reichweite. Vertical lines mark diagnostic $k = 3n$ and $k \neq 3n$ reflections. The asterisks denote 00*l* reflections. Interfering peaks are due, variously, to feldspar, zeolite, calcite, or residuals from the quartz peak stripping procedure. Degrees 2θ, CuKα.

bostratic defects. A correlation coefficient was not calculated because there is no *a priori* basis for assuming a linear relation, or any other specific functional relation between the two variables.

DISCUSSION

*I/S and the crystal structure along c**

The diffraction patterns shown in Figures 1 and 2 lead to the conclusion that either I/S crystallites were never dispersed into fundamental particles, or, if they were, the fundamental particles reaggregated into stacking sequences identical to those in the original rock.

Nadeau *et al.* (1984a) separated fine particle sizes (<0.1 μm) to obtain suspensions that consisted of individual fundamental particles. But the writer prepared oriented and freeze-dried random aggregates from <1 μm fractions. If the present samples are like most <1 μm clay mineral fractions, only small portions of them consist of <0.1 μm material. Therefore, it seems likely that the I/S crystallites in the <1 μm fractions consist mostly of aggregated fundamental particles. The similarity of 00*l* diffraction line breadths for each of the three preparations (Figures 1 and 2) lends strength to this contention.

Even if fundamental particle disaggregation had been accomplished, reaggregation should produce structures that are statistically identical to the original, natural mineral. A megascopic sample of I/S consists of many different optically coherent diffracting arrays (along c^*) that are conveniently called MacEwan crystallites (Al-

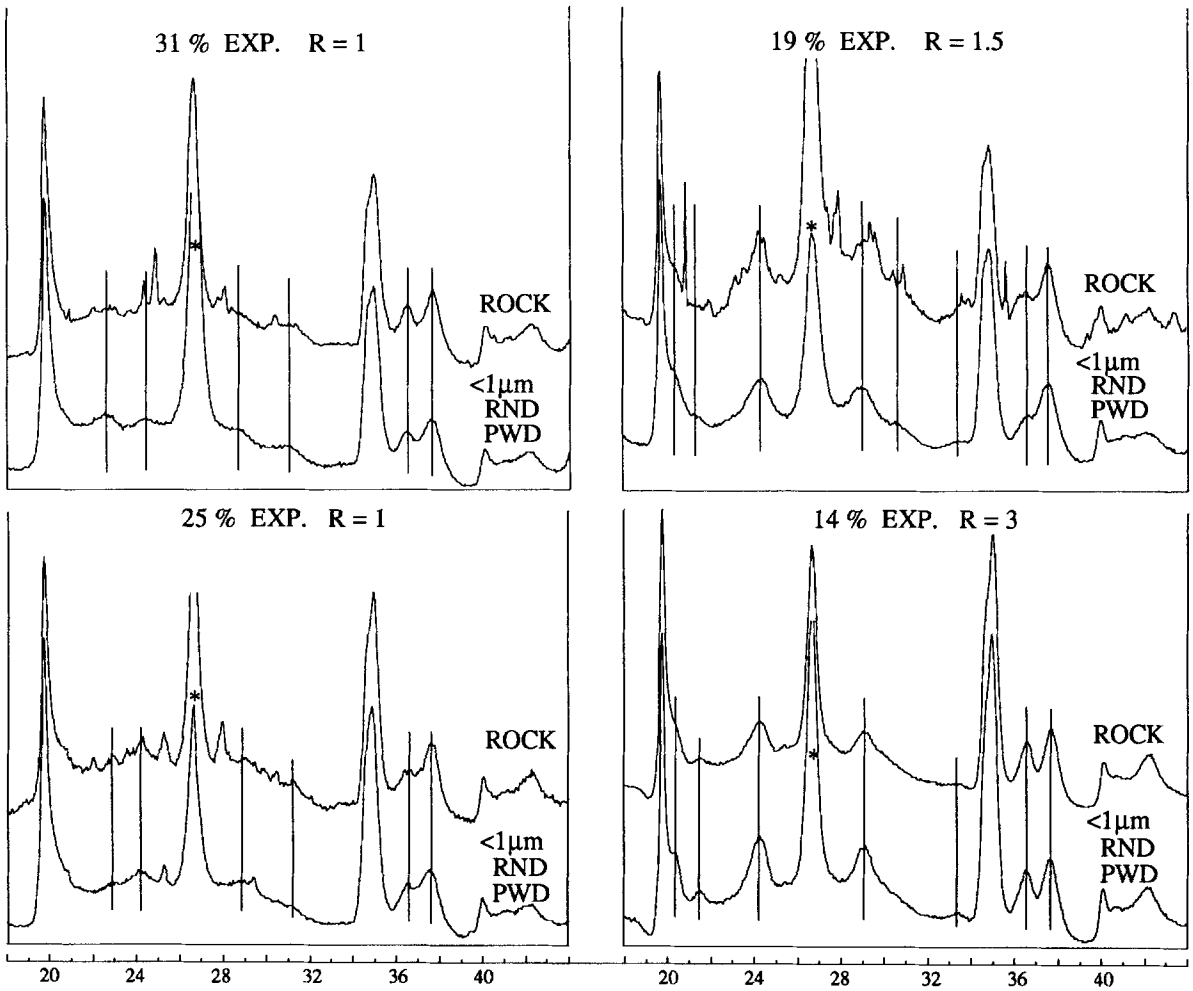

Figure 4. Three-dimensional diffraction patterns of I/S. Comparison between rock fragments (rocks) and <1 μm freeze-dried powders (<1 μm rnd pwd). Captions refer to percent expandability and the Reichweite. Vertical lines mark diagnostic $k = 3n$ and $k \neq 3n$ reflections. The asterisks denote $00l$ reflections. Interfering peaks are due, variously, to feldspar, zeolite, calcite, or residuals from the quartz peak stripping procedure. Degrees 2θ, CuKα.

taner and Bethke, 1988). If, for example, the number of unit silicate layers per MacEwan crystallite is ten, and random interstratification is assumed, there are 2^{10} or about 1000 different kinds of crystallites that cover all possible proportions of illite and smectite layers stacked in all possible permutations. Each of these (except for the two members of the pair produced by simple inversion) produces a unique X-ray diffraction pattern, and the experimental pattern is the sum of all these patterns weighted by the frequency of occurrence of each (Reynolds, 1980). For ordered structures, some stacking sequences are forbidden and are eliminated from the set of possible MacEwan crystallites. We may call this the two-mineral model, illite and smectite.

According to the fundamental particle model, each MacEwan crystallite is a mixture of fundamental particles that contain one or more 2:1 layers, separated at their interfaces by expandable interlayers. The model is conceptually different from the two-mineral model, but it leads to a set of MacEwan crystallites that are almost identical (except for end-effects). Consider, according to the two-mineral model, an I/S that is 30 percent expandable, where Reichweite = 1. There are ideally no 10-Å particles in such an averaged structure, and it consists mostly of 20-Å particles with fewer 30-, still fewer 40-, and perhaps a small number of 50-Å particles. A megascopic powder consists of MacEwan crystallites that collectively represent all combinations and permutations of these four components. An important point needs to be emphasized, namely, that according to the fundamental particle concept, all megascopic I/S minerals, regardless of what heretofore has been called ordering, consist of randomly interstratified stacks of fundamental particles. In a diffrac-

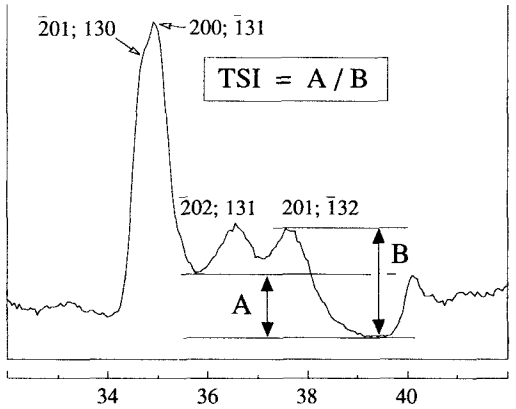

Figure 5. Definition of TSI, the turbostratic index. Degrees 2θ, CuKα.

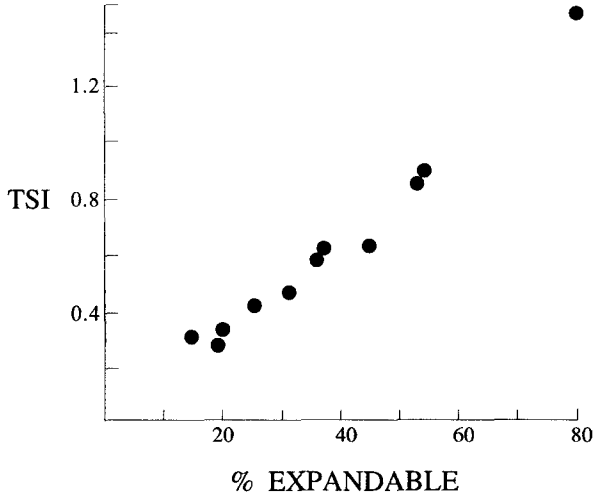

Figure 6. Correlation of the turbostratic index (TSI) with percent expandable layers in I/S.

tometer experiment, diffraction results are averaged over perhaps ten billion MacEwan crystallites that represent hundreds or thousands of different stacking sequences and particle proportions. If the overall, statistically averaged stacking in the original natural material is random, then the writer can conceive of no process or force (excluding the action of Maxwell's demon) that could cause the averaged bulk reaggregated structure to be any different: the reconstructed assemblage will produce a diffraction pattern identical to that of the original, natural material. It does not matter whether or not the original sample was dispersed into fundamental particles: the basal X-ray diffraction patterns will be the same. The same conclusion based on similar reasoning has been suggested by Veblen *et al.* (1990).

The three dimensional structure

Figures 3 and 4 disclose no significant differences between the three-dimensional I/S structures in the bulk rocks and the corresponding <1 μm freeze-dried powders. The relation of Figure 6 suggests why this might be so. Demodulation of the 20*l*, 13*l* peaks into a two-dimensional band is caused by an increase in the frequency of turbostratic displacements which, in the limit, allows diffraction only from single 2:1 silicate layers (except for the 00*l* series which is unaffected by turbostratic stacking). A completely turbostratic structure produces the well-known 20; 13 band shown by many pure smectites (see Figure 3). However, I/S contains fundamental particles that are more than one layer thick, and the 20; 13 band for these will be modulated into the characteristic three-dimensional mica signature (between 34.5 and 39° 2θ) if the fundamental particles contain no internal turbostratic defects although the peaks for which $l > 0$ will be very broad if the fundamental particles are thin.

Figure 6 demonstrates that the TSI increases monotonically with respect to percent expandability. These results suggest that turbostratic dislocations occur at the expandable interfaces between stacks of illite layers (fundamental particles), and that such dislocations are limited to those sites. Of course, the MacEwan crystallites might not have been disaggregated by the sample preparation process used here, but it does not matter. Either possibility leads to identical diffraction patterns between the natural rocks and the corresponding <1 μm freeze-dried random powders, namely, diffraction patterns that depict random interstratification of fundamental particles (internally coherent illite stacks) which are turbostratically translated in and/or rotated about the 001 interfaces between them.

A similar conclusion was reached by Reynolds (1990) based on different kinds of experimental data. For the Zempleni clay, no differences were observed for the positions and intensities of the non-00*l* reflections in the air-dried, dehydrated, and ethylene glycol solvated states. The positions and intensities of the three-dimensional peaks were independent of the average value of d(001), which indicates that coherence exists only across the mica-like interlayer spaces unaffected by dehydration and water and ethylene glycol solvation.

Stacks of illite layers (or illite fundamental particles) that are turbostratically translated (statistically) with respect to each other produce a three-dimensional diffraction pattern of I/S identical to the pattern from a randomly oriented powder of exceedingly thin illite crystallites. This finding opens the possibility for detailed XRD studies of polytypism in the illitic portions of I/S, which otherwise could have been greatly complicated by possible sample-specific variations in (1) rotational stacking angles between fundamental particles, and (2) the three-dimensional atomic structures of the solvated interlayers.

Discrepancy between XRD and HRTEM results

The conclusions of this study seem to conflict with the electron microscope evidence of Ahn and Buseck (1990) and Veblen *et al.* (1990), who show lattice fringe images of large MacEwan crystallites within which turbostratic stacking disorder is minimal. Ahn and Buseck see their results as contradictory to the fundamental particle theory of Nadeau and his co-workers. They argue that the I/S crystallites in the rock have three-dimensional integrity, suggesting that fundamental particles might be artifactual debris produced by the processes of dispersing the I/S clay minerals. The large-area 4.5-Å cross fringes observed by Veblen *et al.* (1990) also suggest three-dimensional integrity within MacEwan crystallites.

Veblen *et al.* (1990) suggest that inter-fundamental particle coherence on the scale observed by HRTEM and small-area selected area electron diffraction could be difficult or impossible to detect by powder XRD studies. They have, thus, anticipated some of the findings reported here. They argue that crystallites with only ten or so silicate layers may produce diffuse two-dimensional bands even if the layers are coherently related. But the present author has made three-dimensional calculations of the shapes of random powder XRD 20; 13 bands as a function of crystallite thickness, and found that even three coherent silicate layers produce significant modulation of this band into a three-dimensional diffraction pattern. If there is a problem of scale, the writer asserts that it is not a problem of scale in the Z direction. Instead, the problem of scale is one of numbers in a statistical average.

An explanation sometimes proposed for differences between XRD and HRTEM findings for disordered crystals is that HRTEM images sample only a few crystallites which may be nonrepresentative of the sample. This suggestion misses the point; namely, no HRTEM image can be representative of the crystallite distribution that the XRD experiment measures, unless, of course, all of the crystallites are identical. In this latter case there is no disorder and no need for an average result. In fact, a representative crystallite does not exist in a disordered mineral, so it is fruitless to search for it. This point is well illustrated by one-dimensional HRTEM studies of I/S. Veblen *et al.* (1990) and Środoń *et al.* (1990) were able to count and average the results for many "illite" and "smectite" layers in HRTEM lattice fringe images and obtain good agreement with the proportions of each as determined by XRD measurements. But none of the individual crystallites measured by them was representative in the sense that it contained, for example, 31 percent smectite and 69 percent illite layers.

From the standpoint of powder XRD theory, it is nonsensical to describe a single displacement as turbostratic. No matter what the displacement between them, there will be a coherent phase effect between two diffracting entities, and it will produce a characteristic diffraction pattern—even between a quartz crystal and a mica flake if diffracting planes of the two rotate simultaneously into the Bragg condition. But if such phase interactions are integrated for many mica-quartz pairs covering all possible separation increments, the cosines of the phase angles times the amplitudes scattered from the two different crystals sum to zero for the assemblage and we are left with the diffraction pattern of a mixture of quartz and mica.

To understand the XRD signature of turbostratic stacking, we have to visualize the sum of diffraction intensities from a very large number of MacEwan crystallites (which for purposes of simplification can be identical except for the fundamental particle displacements within them). Each of these is a single possibility out of the many different interlayer displacements, collectively representing all possible values from zero to plus and minus the unit cell dimension for each displacement site. The powder XRD pattern is the statistically weighted sum of all of these. But a single crystallite of the size observed in HRTEM, regardless of the displacements within it or lack thereof, cannot define the mean and standard deviation of such a statistical distribution.

These arguments suggest that measurements of three-dimensional stacking disorder from powder XRD and HRTEM studies cannot be meaningfully compared at the present time. Studies are required in which many (hundreds of) HRTEM images are recorded and averaged. The X-ray diffraction theorists must produce realistic model shapes of the two- and three-dimensional reflections produced by various kinds and magnitudes of inter-fundamental particle disorder. Veblen *et al.* (1990) have made similar recommendations.

ACKNOWLEDGMENTS

Support for this research was provided by American Chemical Society Grant 23613-AC2. In addition, the writer is indebted to S. P. Altaner and J. Środoń for providing samples used in the study.

REFERENCES

Ahn, J. H. and Buseck, P. R. (1990) Layer-stacking sequences and structural disorder in mixed-layered illite/smectite: Image simulations and HRTEM imaging: *Amer. Mineral.* **75**, 267–275.

Altaner, S. P. and Bethke, C. M. (1988) Interlayer order in illite/smectite: *Amer. Mineral.* **73**, 766–774.

Altaner, S. P., Hower, J., Whitney, G., and Aronson, J. L. (1984) Model for K-bentonite formation: Evidence from zoned K-bentonites in the Disturbed Belt, Montana: *Geology* **12**, 412–425.

Anderson, D. and Reynolds, R. C. (1966) Umiat bentonite: An unusual montmorillonite from Umiat, Alaska: *Amer. Mineral.* **51**, 1443–1456.

Bailey, S. W. (1980) Structures of layer silicates: in *Crystal Structures of Clay Minerals and Their X-Ray Identification,*

G. W. Brindley and G. Brown, eds., Mineralogical Society, London, 1–123.

Bailey, S. W. (1991) Practical notes concerning the X-ray powder diffraction patterns of clay minerals: *Clays & Clay Minerals* **39,** 184–190.

Drits, V. A., Plançon, B. A., Sakharov, B. A., Besson, G., Tsipursky, S. I., and Tschoubar, C. (1984) Diffraction effects calculated for structural models of K-saturated montmorillonite containing different types of defects: *Clay Miner.* **19,** 541–561.

Güven, N. and Burnham, C. W. (1967) The crystal structure of 3*T* muscovite: *Zeit. Kristallogr. Kristallgeom.* **125,** 163–183.

Hinckley, D. N. (1963) Variability of "crystallinity" values among the kaolin deposits of the coastal plain of Georgia and South Carolina: *Clays & Clay Minerals* **11,** 229–235.

Klug, H. P. and Alexander, L. E. (1974) *X-Ray Diffraction Procedures.* J. Wiley and Sons Inc., New York. 996 pp.

Moore, D. M. and Reynolds, R. C. (1989) *X-Ray Diffraction and the Identification and Analysis of Clay Minerals.* Oxford University Press, New York. 332 pp.

Nadeau, P. H. and Reynolds, R. C. (1981) Burial and contact metamorphism in the Mancos Shale: *Clays & Clay Minerals* **29,** 249–259.

Nadeau, P. H., Wilson, M. J., McHardy, W. J., and Tait, J. M. (1984a) Interstratified clays as fundamental particles: *Science* **225,** 923–925.

Nadeau, P. H., Tait, J. M., McHardy, W. J., and Wilson, M. J. (1984b) Interstratified XRD characteristics of physical mixtures of elementary clay particles: *Clay Miner.* **19,** 67–76.

Nadeau, P. H., Wilson, M. J., McHardy, W. J., and Tait, J. M. (1984c) Interparticle diffraction: A new concept for interstratified clays: *Clay Miner.* **19,** 757–769.

Norrish, K. (1954) The swelling of montmorillonite: *Trans. Faraday Soc.* **19,** 120–134.

Ransom, B. and Helgeson, H. C. (1989) Correlation of expandability with mineralogy and layering in mixed-layer clays: *Clays & Clay Minerals* **37,** 189–191.

Reynolds, R. C. (1980) Interstratified clay minerals: in *Crystal Structures of Clay Minerals and Their X-Ray Identification,* G. W. Brindley and G. Brown, eds., Mineralogical Society, London, 249–303.

Reynolds, R. C. (1986) The Lorentz-polarization factor and preferred orientation in oriented clay aggregates: *Clays & Clay Minerals* **34,** 359–367.

Reynolds, R. C. (1990) A preliminary study of order/disorder and polytypism in mixed-layered illite/smectite: in *Programs with Abstracts, 27th Annual Meeting, Clay Minerals Society,* Columbia, Missouri, 1983, p. 105 (abstract).

Reynolds, R. C. and Hower, J. (1970) The nature of interlayering in mixed-layer illite-montmorillonites: *Clays & Clay Minerals* **18,** 25–36.

Smith, D. G. W. (1967) The petrology and mineralogy of some lower Devonian bentonites from Gaspé: *Can. Miner.* **9,** 141–165.

Środoń, J., Andreoli, C., Elsass, F., and Robert, M. (1990) Direct high-resolution transmission microscopic measurement of expandability of mixed-layered illite/smectite in bentonite rock: *Clays & Clay Minerals* **38,** 373–379.

Tsipursky, S. I. and Drits, V. A. (1984) The distribution of octahedral cations in the 2:1 layers of dioctahedral smectites studied by oblique-texture electron diffraction: *Clay Miner.* **19,** 177–193.

Veblen, D. R., Guthrie, G. D., Livi, K. J. T., and Reynolds, R. C. (1990) High-resolution transmission electron microscopy and electron diffraction of mixed-layer illite/smectite: Experimental results: *Clays & Clay Minerals* **38,** 1–13.

(Received 8 January 1992; accepted 1 June 1992; Ms. 2174)